American Journal of Pathology, Vol. 163, No. 5, November 2003

Abnormalities of Basement Membrane on Blood Vessels and Endothelial Sprouts in Tumors

Peter Baluk, Shunichi Morikawa, Amy Haskell, Michael Mancuso, and Donald M. McDonald

From the Cardiovascular Research Institute, Comprehensive Cancer Center, and the Department of Anatomy, University of California, San Francisco, California

Often described as incomplete or absent, the basement membrane of blood vessels in tumors has attracted renewed attention as a source of angiogenic and anti-angiogenic molecules, site of growth factor binding, participant in angiogenesis, and potential target in cancer therapy. This study evaluated the composition, extent, and structural integrity of the basement membrane on blood vessels in three mouse tumor models: spontaneous RIP-Tag2 pancreatic islet tumors, MCa-IV mammary carcinomas, and Lewis lung carcinomas. Tumor vessels were identified by immunohistochemical staining for the endothelial cell markers CD31, endoglin (CD105), vascular endothelial growth factor receptor-2, and integrin alpha5 (CD49e). Confocal microscopic studies revealed that basement membrane identified by type IV collagen immunoreactivity covered >99.9% of the surface of blood vessels in the three tumors, just as in normal pancreatic islets. Laminin, entactin/nidogen, and fibronectin immunoreactivities were similarly ubiquitous on tumor vessels. Holes in the basement membrane, found by analyzing 1-μm confocal optical sections, were <2.5 μm in diameter and involved only 0.03% of the vessel surface. Despite the extensive vessel coverage, the basement membrane had conspicuous structural abnormalities, including a loose association with endothelial cells and pericytes, broad extensions away from the vessel wall, and multiple layers visible by electron microscopy. Type IV collagen-immunoreactive sleeves were also present on endothelial sprouts, supporting the idea that basement membrane is present where sprouts grow and regress. These findings indicate that basement membrane covers most tumor vessels but has profound structural abnormalities, consistent with the dynamic nature of endothelial cells and pericytes in tumors. ***(Am J Pathol 2003, 163:1801–1815)***

Blood vessels of tumors have multiple structural and functional abnormalities. Their unusual leakiness, potential for rapid growth and remodeling, and expression of distinctive surface molecules not only are responsible for mediating hematogenous spread of tumor cells and maintaining the unusual microenvironment of tumors but also are key to the efficacy of targeted tumor therapy.[1–4] Like normal blood vessels, tumor vessels consist of endothelial cells, mural cells (pericytes or smooth muscle cells), and their enveloping basement membrane. The nature and severity of the abnormalities in the endothelial cells and pericytes are described in numerous reports,[5–11] but the abnormalities of the basement membrane have received less attention. The identification of basement membrane as a source of angiogenic and anti-angiogenic factors and as a potential diagnostic or therapeutic target in cancer further increases the importance of this component of the wall of tumor vessels.[12–15]

The vascular basement membrane is a dynamic, self-assembled layer of proteins, glycoproteins, and proteoglycans formed by and enveloping endothelial cells and pericytes of blood vessels. Major constituents include type IV collagen, laminin, entactin/nidogen, fibronectin, and the heparan-sulfate proteoglycan perlecan.[16] Basement membrane on blood vessels can be readily identified by immunohistochemical staining of the component proteins.[17,18] Fine structural features of basement membrane (basal lamina), including the ~30- to 40-nm-thick electron-lucent lamina rara next to the cell membrane and the ~50- to 80-nm-thick outer electron dense lamina densa, are evident by electron microscopy (EM).[19]

Conventional wisdom predicts that the basement membrane of endothelial cells is degraded during angiogenesis to enable sprout formation and endothelial cell migration.[20] Alternatively, it is possible that the basement membrane does not disappear during angiogenesis but instead remodels continuously as endothelial sprouts form and new vessels grow.[21–23]

The status of the basement membrane on blood vessels in tumors is unclear. Many morphological studies

Supported in part by the National Institutes of Health (grants HL-24136 and HL-59157 from the National Heart, Lung, and Blood Institute) and Munich Biotech AG, Munich, Germany.

D. M. M. has an equity position in Munich Biotech.

P. B. and S. M. contributed equally to this work.

Accepted for publication July 16, 2003.

Present address of S. M.: Department of Anatomy and Developmental Biology, Tokyo Women's Medical University, 8-1 Kawada-Cho, Shinjuku, Tokyo 162-8666 Japan. E-mail: shun@research.twmu.ac.jp.

Address reprint requests to Donald M. McDonald, Department of Anatomy, S1363, University of California, 513 Parnassus Ave., San Francisco, CA 94143-0452. E-mail: dmcd@itsa.ucsf.edu.

have reported that the basement membrane of tumor vessels is incomplete or absent,[17,24–27] yet other studies suggest that it is present but morphologically abnormal.[28] These discrepancies probably result from the use of different approaches. Some reports of defective or absent basement membrane on tumor vessels are based on observations made by transmission EM. The high resolution of this approach can reveal tiny abnormalities but may miss unstained components and the overall amount of coverage. Light microscopic immunohistochemistry can detect the specific protein components of basement membrane and readily provide an overview despite its lower spatial resolution. Although this approach is frequently used to visualize basement membrane in tumors,[17,18,29,30] one of the challenges is to distinguish the basement membrane of blood vessels from that associated with tumor cells or other components. Co-localization of markers for basement membrane and endothelial cells helps in this regard. However, the distribution and extent of coverage of basement membrane proteins specifically associated with endothelial cells and pericytes has been examined in relatively few tumors.[28]

The goal of the present study was to characterize the completeness and abnormalities of the basement membrane of blood vessels and endothelial sprouts in mouse tumor models. Specifically, we sought to: 1) determine the distribution and extent of coverage of vascular basement membrane in tumors by using immunohistochemistry to co-localize multiple markers of endothelial cells and basement membrane; 2) examine the relationship between vascular basement membrane and endothelial cells and pericytes in tumors; and 3) determine whether basement membrane is associated with endothelial sprouts. To this end, we studied three tumor models in mice: spontaneous pancreatic islet tumors in RIP-Tag2 transgenic mice and implanted syngeneic MCa-IV mouse mammary carcinomas and Lewis lung carcinomas.[10] Basement membrane, identified by type IV collagen, laminin, fibronectin, or entactin/nidogen immunoreactivity, was co-localized with endothelial cells identified by CD31, endoglin (CD105), vascular endothelial growth factor receptor-2 (VEGFR-2), or integrin alpha5 (CD49e) immunoreactivity and with pericytes marked by α-smooth muscle actin (α-SMA) immunoreactivity. Three-dimensional views were obtained by examining 80-μm-thick sections by confocal microscopy. Ultrastructural relationships were examined by transmission EM.

Materials and Methods

Animals and Preparation of Tumors

Spontaneous pancreatic islet cell tumors were examined in 10-week-old RIP-Tag2 transgenic mice with a C57BL/6 background.[10] Normal pancreatic islets were examined in wild-type C57BL/6 mice. Implanted MCa-IV mouse mammary carcinomas (Massachusetts General Hospital, Boston, MA) and Lewis lung carcinomas (American Type Culture Collection, Rockville, MD) were studied in syngeneic male C3H and C57BL/6 mice, respectively, 2 to 3 weeks after implantation when they were 5 to 10 mm in diameter.[10] All experimental procedures were approved by the Committee on Animal Research at the University of California, San Francisco, CA.

Immunofluorescence Histochemistry

Mice were anesthetized with ketamine (87 mg/kg) plus xylazine (13 mg/kg) injected intramuscularly. The chest was opened rapidly, and the vasculature was perfused for 3 minutes at a pressure of 120 mmHg with fixative [4% paraformaldehyde in 0.1 mol/L phosphate-buffered saline (PBS), pH 7.4; Sigma Chemical Co., St. Louis, MO] from an 18-gauge cannula inserted into the aorta via an incision in the left ventricle. Blood and fixative exited through an opening in the right atrium. After the perfusion, the entire pancreas or implanted tumor with overlying dorsal skin was removed and placed into fixative for 2 hours at 4°C. Specimens were then rinsed several times with PBS, embedded in 10% agarose for Vibratome sectioning or infiltrated overnight with 30% sucrose, and frozen for cryostat sectioning.

Vibratome or cryostat sections 80 μm in thickness were incubated in 5% normal goat serum (Jackson ImmunoResearch, Inc., West Grove, PA) in PBS containing 0.3% Triton X-100 (Sigma), 0.2% bovine serum albumin (Sigma), and 0.01% thimerosal (Sigma) for 1 hour at room temperature to block nonspecific antibody binding. Next, the sections were incubated for 12 to 15 hours at room temperature in humidified chambers in combinations of two or three primary antibodies diluted in the medium described above. Endothelial cells were identified with antibodies to CD31 [PECAM-1, rat monoclonal, clone MEC 13.3, 1:500 (BD Pharmingen, San Diego, CA) or hamster monoclonal, clone 2H8, 1:500 (Chemicon, Temecula, CA)], endoglin (CD105, rat monoclonal, clone MJ7/18, 1:400; BD Pharmingen), VEGFR-2 (rabbit polyclonal T014, 1:2000; a kind gift from Dr. Rolf A. Brekken, Hope Heart Institute, Seattle, WA), or integrin alpha5 subunit (CD49e, rat monoclonal, clone 5H10-17, 1:400; BD Pharmingen). Pericytes were identified with anti-α-SMA (α-SMA, Cy3-conjugated mouse monoclonal, clone 1A4, 1:1000; Sigma). Basement membrane was identified with antibodies to type IV collagen (rabbit polyclonal, 1:10,000; Cosmo Bio Co. Ltd., Tokyo, Japan), laminin (rabbit polyclonal antibody that recognizes most laminin isoforms, 1:2000; Chemicon), entactin/nidogen (rat monoclonal, clone MAB1946, 1:1000; Chemicon), or fibronectin (rabbit polyclonal, 1:2000; Sigma). After several rinses with PBS, specimens were incubated for 6 hours at room temperature with fluorescent (fluorescein isothiocyanate, Cy3, or Cy5) secondary antibodies (goat anti-rat, anti-hamster, or anti-rabbit; Jackson ImmunoResearch) diluted 1:400 in PBS containing 0.3% Triton X-100 followed by several rinses in PBS. Finally specimens were mounted in Vectashield (Vector Laboratories, Burlingame, CA) and were examined with a Zeiss Axiophot fluorescence microscope equipped with single, dual, and triple fluorescence filters and a low-light, three-

chip CoolCam CCD camera (SciMeasure Analytical Systems, Atlanta, GA) and a Zeiss LSM 410 or LSM 510 confocal microscope (Carl Zeiss, Thornwood, NY) with three photomultiplier tubes. Images were saved as digital files.

Transmission EM

Tumors were fixed for transmission EM by vascular perfusion as for immunohistochemistry except the fixative contained 3% glutaraldehyde, 0.05% calcium chloride, 4% polyvinylpyrrolidone, and 1% sucrose in 75 mmol/L sodium cacodylate buffer, pH 7.1. After the 5-minute perfusion, tissues were removed and fixed overnight or longer at 4°C, and then sections 80 μm in thickness were cut with a Vibratome (TPI, St. Louis, MO). Sections were treated with 1% osmium tetroxide in 100 mmol/L cacodylate buffer (pH 7.2) for 2 hours at 4°C and then with 2% aqueous uranyl acetate for 48 hours at 37°C, dehydrated in acetone, and embedded in epoxy resin. Sections, 0.5 μm in thickness, were stained with toluidine blue for light microscopy, and sections 50 to 100 nm in thickness were stained with 0.8% lead citrate in 0.2 N NaOH and examined with a Zeiss EM 10-C electron microscope.

Morphometric Measurements

The extent of coverage of blood vessels by type IV collagen immunoreactivity was examined in 1-μm-thick optical sections made by confocal microscopy of 80-μm-thick tissue sections. Confocal images of cross-sections of 25 vessels were prepared from specimens of normal pancreatic islets and non-necrotic regions of each type of tumor ($n = 4$ mice per group). Regions of blood vessel profiles lacking type IV collagen immunoreactivity were counted and measured, and the percentage of profiles with such defects was calculated. The perimeters of CD31-immunoreactive endothelial cells and type IV collagen-immunoreactive basement membrane were measured using a digitizing tablet.[10] The percentage of vessel wall coverage by basement membrane was calculated as the ratio of the length of type IV collagen staining to total vessel perimeter reflected by CD31 staining. The length of CD31-immunoreactive endothelial sprouts, identified as thin, tapered, blind-ending projections away from the main axis of vessels, was measured, as was the length of their coat of type IV collagen immunoreactivity. Values are expressed as means ± SEM (SE). The significance of differences between means was assessed by analysis of variance followed by the Bonferroni/Dunn test for multiple comparisons, with statistical significance judged as $P < 0.05$.

Results

Distribution of Basement Membrane Proteins on Blood Vessels in Tumors

Vascular basement membrane was identified by co-localization of immunohistochemical markers of endothelial cells and basement membrane. To determine which immunohistochemical marker was most effective for staining endothelial cells in the tumor models, we first compared two different antibodies to CD31 and then paired the better one with antibodies to endoglin (CD105), VEGFR-2, or integrin alpha5 (CD49e). Both antibodies to CD31 stained the same population of tumor vessels. Similarly, antibodies to CD31 primarily co-localized with the other three markers, but scattered vessels stained more strongly with one antibody or another (Figure 1). Overall, antibodies to CD31 stained the largest number of vessels. CD105 and VEGFR-2 were approximately the same as CD31 (Figure 1; A to C and D to F); CD49e stained slightly fewer vessels (Figure 1; G to I).

Immunohistochemical staining of type IV collagen, laminin, fibronectin, and entactin/nidogen immunoreactivities uniformly stained the blood vessels in RIP-Tag2 pancreatic tumors, MCa-IV mammary carcinomas, and Lewis lung carcinomas (Figure 2; A to C, G, H). Double staining documented the uniform co-localization of basement membrane proteins (Figure 2; A to C) and CD31 immunoreactivity of endothelial cells (Figure 2; D to F). Adjacent sections stained with different antibodies showed that the immunoreactivities of multiple basement membrane proteins co-localized with one another on tumor vessels (Figure 2; A to C). Type IV collagen immunoreactivity strongly defined the vascular basement membrane (Figure 2A); other regions of the tumors were stained weakly or not at all. Laminin (Figure 2B), fibronectin (Figure 2C), and entactin/nidogen (Figure 2H) immunoreactivities clearly marked the vascular basement membrane but also stained some tumor cells or stromal elements. Because type IV collagen immunoreactivity, of the four markers used, was the most selective for vascular basement membrane in these tumors, it was used for further studies.

In normal pancreatic islets, type IV collagen immunoreactivity co-localized with CD31 immunoreactivity in all blood vessels and thus gave an accurate representation of the vascular architecture (Figure 3, A and B); however, type IV collagen immunoreactivity also surrounded acini of the normal exocrine pancreas (Figure 3A, arrows). In 80-μm-thick sections of the three tumors, the type IV collagen sleeves disclosed the irregularity and tortuosity of the tumor vessels (Figure 3, C and D). On some tumor vessels, the region of type IV collagen immunoreactivity was appreciably larger than the region CD31 immunoreactivity, suggesting that some regions of vascular basement membrane were not tightly associated with endothelial cells (Figure 3, C and D, arrowheads). No blood vessel identified by CD31 immunoreactivity in any of the tumors completely lacked type IV collagen immunoreactivity.

Abnormalities of Basement Membrane on Blood Vessels in Tumors

Confocal microscopic examination of 1-μm optical cross-sections of blood vessels in normal pancreatic islets showed a continuous, smooth and uniform layer of type

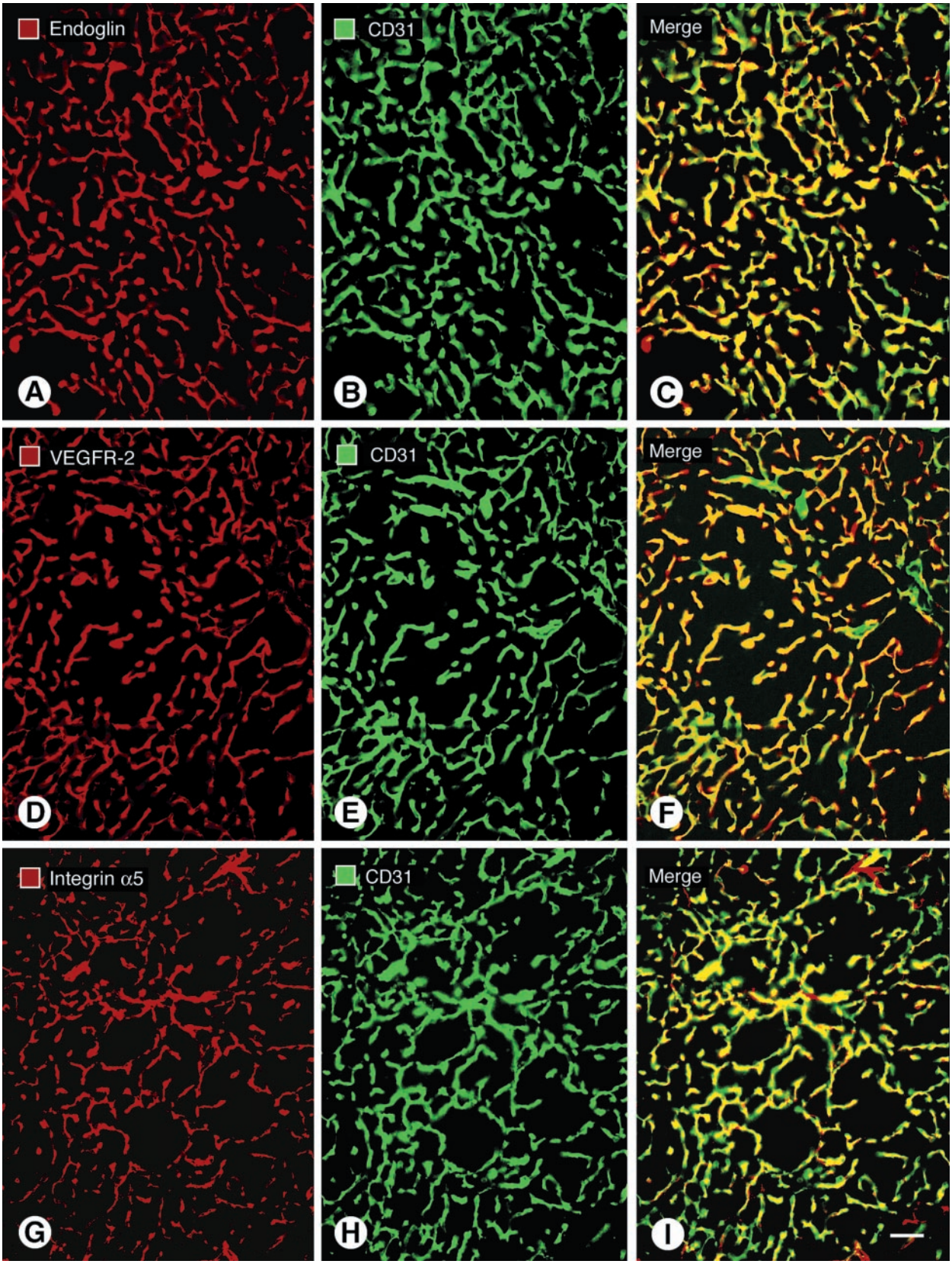

Figure 1. Fluorescence micrographs showing blood vessels in RIP-Tag2 tumors double-stained for the endothelial cell markers endoglin (**A**); VEGFR-2 (**D**); or integrin alpha5 (**G**), shown in red; and CD31 immunoreactivity (**B**, **E**, **H**), shown in green. CD31 immunoreactivity primarily co-localizes with the other markers, but the overlap is not perfect (**C**, **F**, **I**). The most complete co-localization, indicated by yellow fluorescence in the merged image, is found with endoglin (**C**) and VEGFR-2 (**F**). Some vessels marked by CD31 have little or no integrin alpha5 immunoreactivity, as indicated by green fluorescence in the merged image (**I**). Few vessels lack CD31 immunoreactivity, as indicated by red fluorescence in merged images (**C**, **F**, **I**). Scale bar, 50 μm (**A–I**).

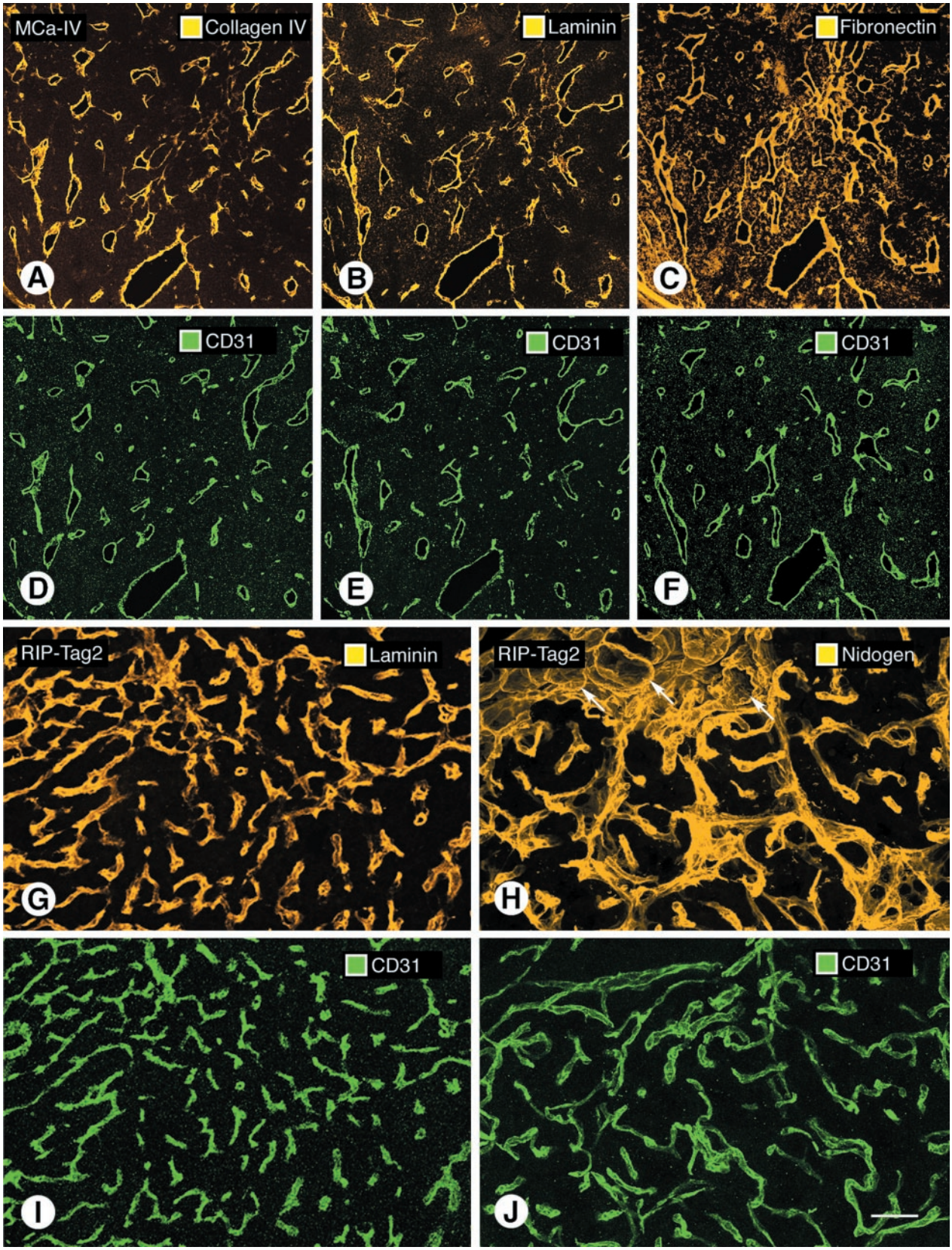

Figure 2. Confocal microscopic images of vascular basement membrane stained by type IV collagen (**A**), laminin (**B**), and fibronectin (**C**) immunoreactivities in sequential sections of MCa-IV tumor. All three basement membrane proteins co-localize with CD31 immunoreactivity in the same sections (**D–F**). Type IV collagen immunoreactivity is primarily restricted to blood vessels in these tumors, but laminin and fibronectin immunoreactivities are also present elsewhere in the tumors. Laminin (**G**) and entactin/nidogen (**H**) immunoreactivities and corresponding CD31 immunoreactivity (**I**, **J**) are shown associated with blood vessels in RIP-Tag2 tumors. **Arrows** in **H** mark exocrine pancreatic acini outlined by entactin/nidogen immunoreactivity. Scale bars: 170 μm (**A–F**); 50 μm (**G–J**).

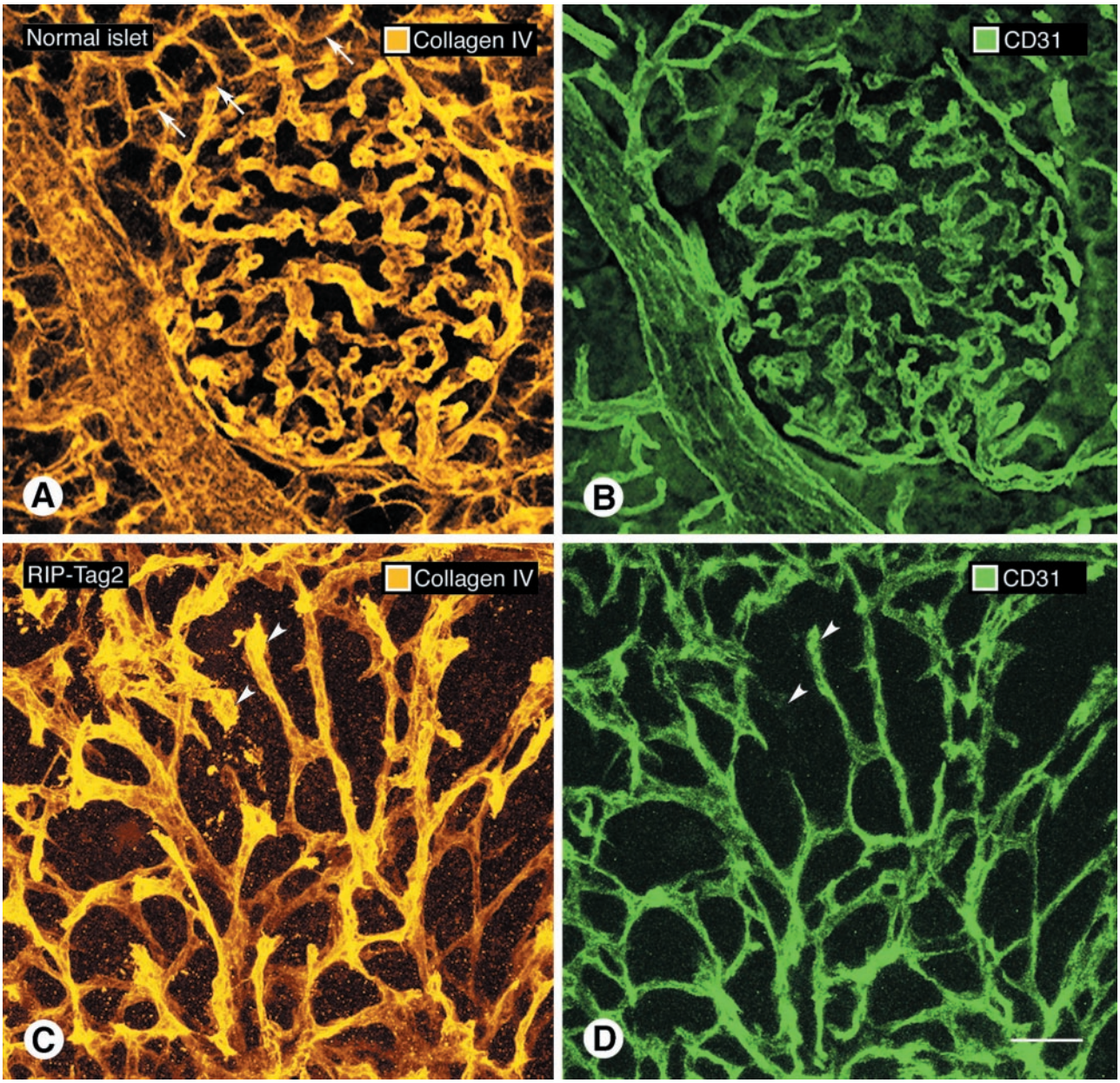

Figure 3. Confocal microscopic images of type IV collagen immunoreactivity of basement membrane (**A**, **C**) and CD31 immunoreactivity of endothelial cells (**B**, **D**) in normal pancreatic islet of wild-type mouse (**A**, **B**) and in RIP-Tag2 tumor (**C**, **D**). In both cases, all CD31-immunoreactive vessels co-localize with type IV collagen immunoreactivity. Tumor vessels are more irregular and tortuous but still have a uniform envelopment of type IV collagen immunoreactivity. **Arrowheads** mark tumor vessels where type IV collagen staining (**C**) is broader or more prominent than the corresponding CD31 immunoreactivity (**D**), suggestive of a loose association with endothelial cells. **Arrows** in **A** point to exocrine pancreatic acini outlined by type IV collagen immunoreactivity. Scale bar, 50 μm (**A–D**).

IV collagen immunoreactivity that faithfully matched the CD31 immunoreactivity of endothelial cells (Figure 4A). Quantitative analysis of 100 vessels in normal islets found only one small defect in the type IV collagen immunoreactivity and >99.9% coverage (Table 1). Corresponding 1-μm optical sections of RIP-Tag2 tumor vessels showed the layer of type IV collagen to be variable in thickness and to have conspicuous surface projections and other irregularities that were never seen in normal vessels (Figure 4, B and C, arrows). Yet the layer of type IV collagen on tumor vessels was nearly complete (Figure 4, B and C). Measurements revealed that type IV collagen immunoreactivity covered >99.9% of the endothelial surface; only 0.03% of the vessel surface lacked staining (Table 1). One defect, ~0.4 μm in diameter, was found in sections of 100 vessel profiles in RIP-Tag2 tumors (Figure 4, B and C). MCa-IV breast carcinomas had more basement membrane abnormalities (Figure 4; D to F); but even here defects were detected in only 2% of the 1-μm optical sections examined, and the largest was 2.5 μm in diameter (Table 1). Blood vessels of Lewis lung carcinomas had basement membrane defects approximately the same size and frequency as those in RIP-Tag tumors (Figure 4G, Table 1). Basement membrane defects

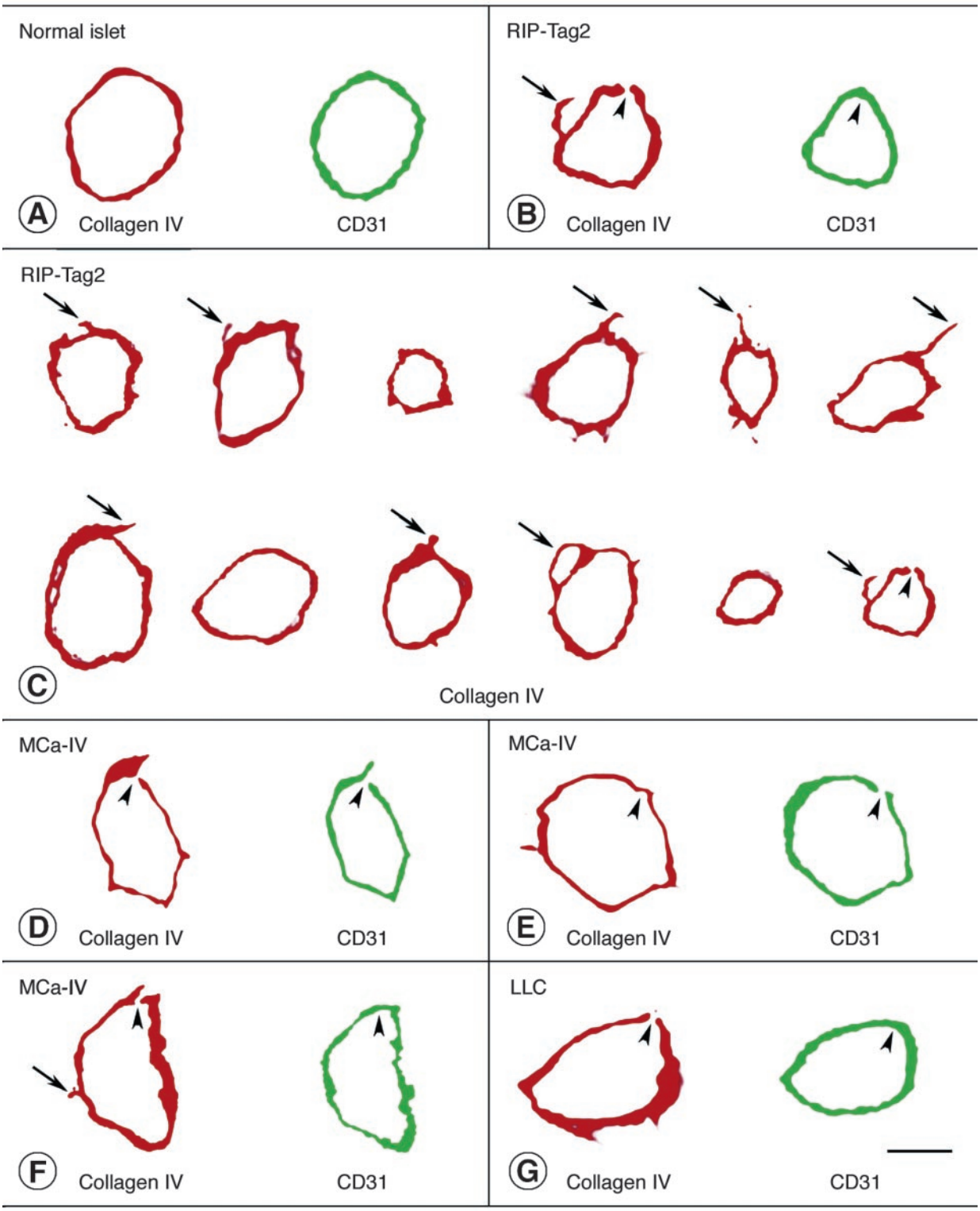

Figure 4. Type IV collagen (red) and CD31 immunoreactivities (rat clone MEC13.3 anti-mouse, green) viewed in two-dimensional projections of 1-μm confocal microscopic optical cross-sections of vessels in normal pancreatic islets (**A**), RIP-Tag2 tumors (**B**, **C**), MCa-IV breast carcinomas (**D–F**), and Lewis lung carcinoma (**G**). Physical section thickness, 80 μm. Type IV collagen immunoreactivity completely envelops most vessels. **Arrows** mark regions of type IV collagen immunoreactivity that extend beyond the CD31-immunoreactive perimeter of tumor vessels. **Arrowheads** mark tiny defects (0.3 to 2.5 μm in diameter) in type IV collagen immunoreactivity and/or CD31 immunoreactivity of vessels in the three types of tumor, as detailed in Table 1. There are several reasons why CD31 immunoreactivity of endothelial cells appears as a single band instead of two discrete (luminal and abluminal) plasma membranes in these images. To visualize the immunofluorescence in 1-μm optical sections of endothelial cells, the confocal signal was amplified to a point plasma membranes appear wider than they really are. The apparent widening of the membranes is exaggerated by slight tilting from vertical of vessels not cut precisely in cross-section. The separation of the two membranes is less than the thickness of the optical sections (except in the region of the nucleus) and is of the same order of magnitude as the resolution of the ×40 objective lens. Because of the interaction of these factors, the width of the signal from both membranes blurs the space between them, and they fuse into one fluorescent band. Scale bars: 5 μm (**A**, **B**, **G**); 7.5 μm (**C**); 45 μm (**D–F**).

Table 1. Extent of Basement Membrane Coverage of Normal Blood Vessels and Tumor Vessels

	Normal pancreatic islets	RIP-Tag2 pancreatic islet tumors	MCa-IV mammary carcinomas	Lewis lung carcinomas
Percent of vessel profiles entirely covered by type IV collagen immunoreactivity	99 ± 1%	99 ± 1%	98 ± 1%	99 ± 1%
Number of defects in type IV collagen immunoreactivity in 100-vessel sample	1	1	3	1
Size of defects in type IV collagen immunoreactivity	1.0 μm	0.3 μm	1.3, 2.1, 2.5 μm	0.4 μm
Percent of vessel coverage by type IV collagen immunoreactivity	> 99.9%	> 99.9%	> 99.9%	> 99.9%

Basement membrane was identified by type IV collagen immunoreactivity and corresponding endothelial cells were visualized by CD31 immunoreactivity in 80-μm-thick sections of normal pancreatic islets and three mouse tumor models. Perimeters of type IV collagen and CD31 staining on vessels cut perpendicular to their longitudinal axis were measured in 1-μm confocal optical sections. Proportion of vessels without basement membrane defects was determined from the percent of profiles entirely surrounded by type IV collagen staining. Percent of basement membrane coverage was calculated as the ratio of the length of type IV collagen staining to total vessel perimeter reflected by CD31 staining. One hundred vessel profiles were measured in each model (25 profiles per mouse; four mice per model). Values are expressed as means ± SE, (n = 4). Cumulative vessel perimeters for each model were 2070 μm for normal pancreatic islets, 2320 μm for RIP-Tag2 tumors, 11315 μm for MCa-IV carcinomas, and 8343 μm for Lewis lung carcinomas. Differences in vessel perimeter among the three tumors reflect documented differences in mean vessel size.[7,10] Defects in type IV collagen staining, measured in 1-μm optical sections, constituted ≈ 0.05% in normal islet blood vessels and 0.01%, 0.05%, and 0.005% (overall value = 0.03%) of the vessel surface in the three tumors.

smaller than ~0.1 μm probably would not be detected by this approach.

One of the defects in type IV collagen immunoreactivity identified in 1-μm optical sections coincided with a similar defect in CD31 immunoreactivity (Figure 4D). This presumably represents a hole in the endothelium and would be a potential site for extravasation.[7] Another defect in CD31 immunoreactivity was next to continuous type IV collagen staining (Figure 4E). Other defects in the layer of type IV collagen were next to regions of uninterrupted CD31 staining (Figure 4; B, F, and G).

Co-localization of type IV collagen, CD31, and α-SMA immunoreactivities in confocal optical cross-sections of blood vessels of normal skin in the region of tumor implantation revealed a uniform sleeve of type IV collagen that closely enveloped endothelial cells and pericytes, forming a tightly packed sandwich in which no spaces were visible between the layers (Figure 5; A to C). The situation was conspicuously different in tumor vessels. Here, spaces separated layers of type IV collagen, CD31, and α-SMA immunoreactivities, indicative of a loose association of basement membrane, endothelial cells, and pericytes (Figure 5; D to F). Redundant segments of type IV collagen immunoreactivity extended away from the endothelium into the tumor stroma (Figure 5G). Some of these projections surrounded pericyte processes (Figure 5G, arrows); others were seemingly not associated with endothelial cells or pericytes (Figure 5G, arrowheads).

Transmission EM studies confirmed that the basement membrane of tumor vessels was primarily continuous but conspicuously abnormal (Figure 6; A to C). On some vessels in MCa-IV tumors (Figure 6A, arrows) and RIP-Tag2 tumors (Figure 6B, C, arrows), multiple distinct layers of basement membrane were present, suggesting that the forming cells had undergone repeated remodeling. EM images also confirmed the loose association of basement membrane with endothelial cells and pericytes (Figure 6A, arrows). Basement membrane on clusters of tumor cells was more compact and morphologically much simpler than that on blood vessels, appearing as a single thin layer closely apposed to the outer surface of cell clusters (Figure 6A, arrowheads).

Basement Membrane on Endothelial Sprouts in Tumors

The question of whether endothelial sprouts on tumor vessels are covered by basement membrane was addressed by examining the type IV collagen immunoreactivity of 40 CD31-immunoreactive sprouts in each of the three tumor models. Sprouts, which were identified as thin CD31-positive processes extending away from the main axis of tumor vessels, ranged in length from 5 to 61 μm (Figure 7, Table 2). Such sprouts were not detected on blood vessels of normal islets. The analysis revealed that most endothelial sprouts had type IV collagen immunoreactivity along their entire length. Indeed, the length of the type IV collagen immunoreactivity of sprouts averaged 75%, 70%, and 53% longer than the CD31-positive region in the tumor models (Table 2). Only 5% of the sprouts had naked regions, ~5 μm in length, that lacked type IV collagen immunoreactivity at their tip (Table 2).

Pericyte processes accompanied most sprouts. These processes, as judged by α-SMA immunoreactivity along sprouts, were approximately the same length as the type IV collagen immunoreactivity, and were considerably longer (80%, 62%, and 38%, respectively) than the CD31-positive region of sprouts (Table 2). Consequently, the distal-most 10 to 20 μm of most sprouts consisted of a pericyte process covered by basement membrane but no associated CD31 immunoreactivity.

Discussion

This study identified and characterized abnormalities of the basement membrane of tumor vessels in three mouse tumor models: spontaneous pancreatic islet cell tumors in RIP-Tag2 mice, MCa-IV breast carcinomas, and Lewis

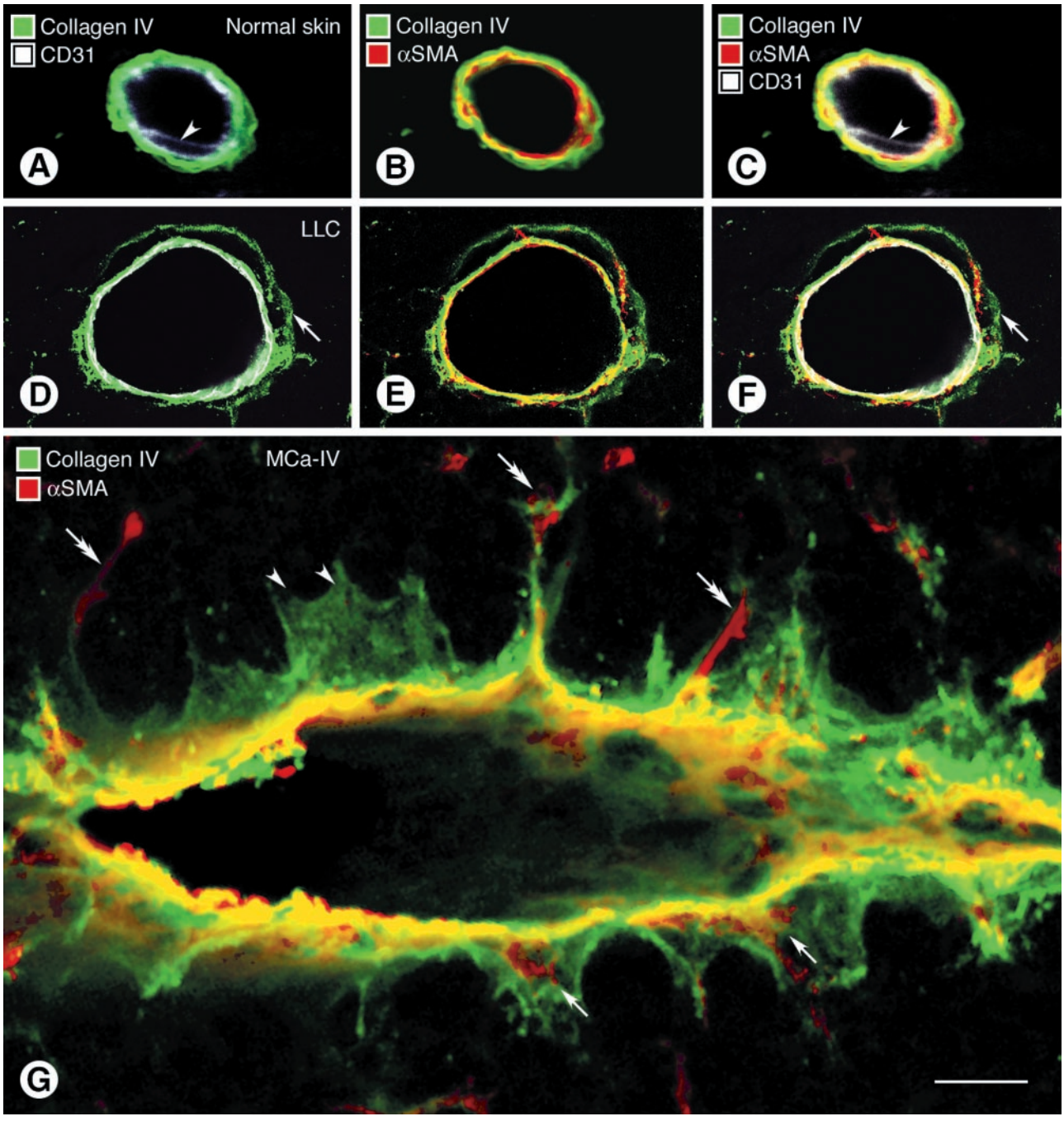

Figure 5. Confocal microscopic images comparing wall structure of 5-μm-thick optical sections of vessels in normal skin (**A–C**) and Lewis lung carcinoma (**D–F**, LLC) triple-stained for CD31, α-SMA, and type IV collagen immunoreactivities. Type IV collagen staining in the normal venule is closely apposed to CD31-immunoreactive endothelial cells (**A**) and α-SMA-immunoreactive pericytes (**B**). All three markers form a tight sandwich (**C**). **Arrowheads** mark endothelial cell nucleus. In the tumor vessel a layer of type IV collagen immunoreactivity extends well beyond the endothelial cells (**D–F**, **arrows**) and in some regions co-localizes with α-SMA-positive pericytes (**E**). A composite view (**F**) shows that the cell layers and basement membrane are separated by spaces (black). CD31 staining in some images (**A**, **C**, **D**, **F**) appears somewhat diffuse and not precisely limited to the plasma membrane for the reasons mentioned in the legend for Figure 4. In **G**, multiple basement membrane abnormalities are shown in an oblique section through a vessel in MCa-IV breast carcinoma, double-stained for type IV collagen (green) and α-SMA (red) immunoreactivities, with regions of greatest overlap appearing yellow. Type IV collagen immunoreactivity spreads loosely from the vessel wall and penetrates the surrounding stroma (black). Extensions of type IV collagen immunoreactivity envelop α-SMA-immunoreactive pericytes in some regions (**arrows**) but not in others (**arrowheads**). Some α-SMA-immunoreactive cell processes extend away from the vessel wall (**double arrows**). Scale bar, 10 μm (**A–G**).

lung carcinomas. In these tumors, type IV collagen, laminin, entactin/nidogen, and fibronectin immunoreactivities all enveloped tumor vessels. The amount of nonvascular staining varied widely among the markers, with type IV collagen immunoreactivity having the most selective association with blood vessels. More than 99% of the vascular surface in all three tumors was covered by type IV collagen staining. Basement membrane defects lacking type IV collagen were focal, uncommon, and measured <2.5 μm in diameter. However, multiple abnormalities in

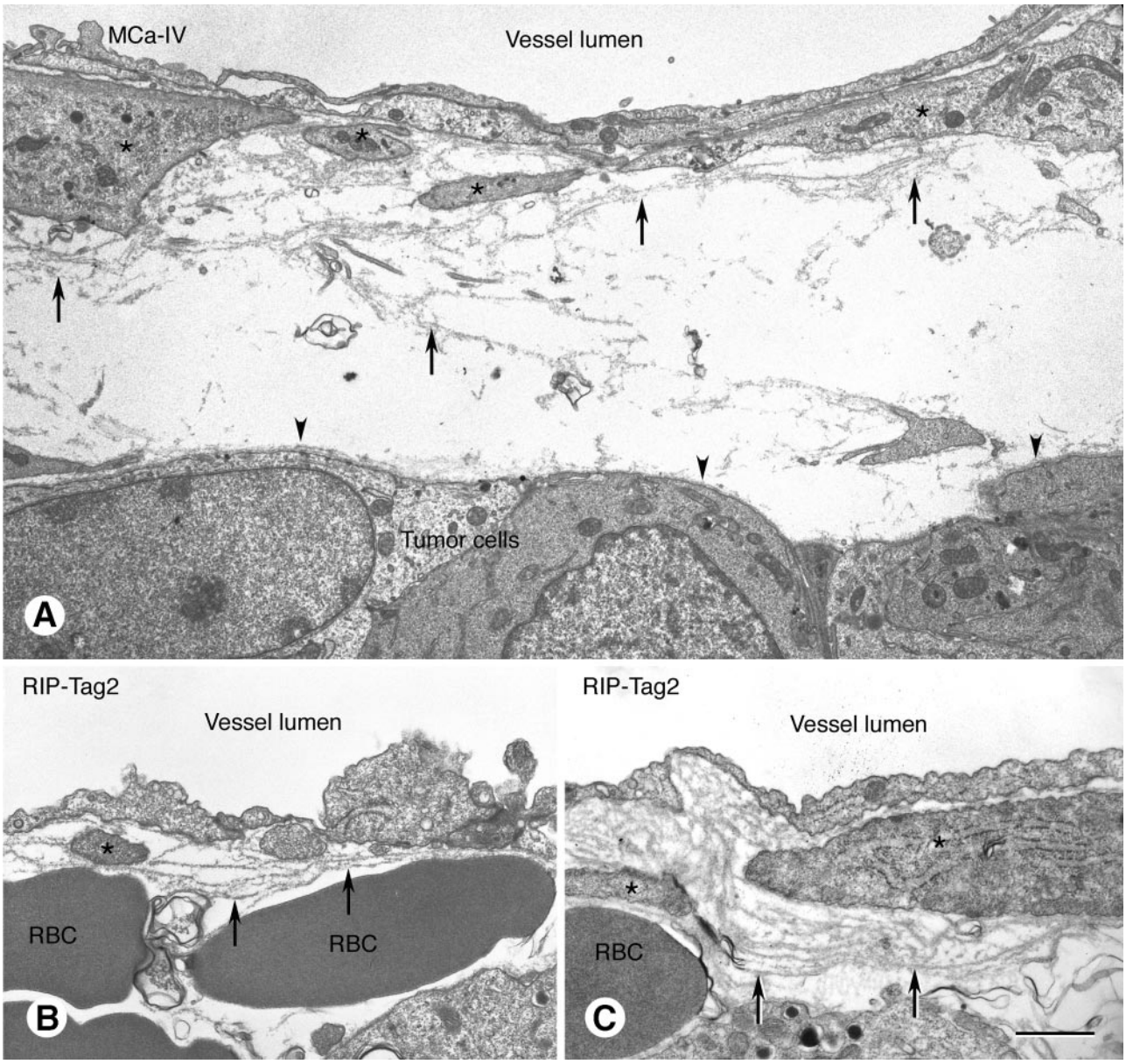

Figure 6. Transmission electron micrographs of blood vessels in MCa-IV mammary carcinoma (**A**) and RIP-Tag2 tumor (**B**, **C**) with basement membrane (**arrows**) that is structurally abnormal but provides complete vessel coverage. Endothelial cells line the vessel lumen. Pericytes are marked by **asterisks**. Basement membrane is loosely associated with endothelial cells and pericytes and in some regions extends away from the vessel wall (**A**, **arrows**). Some regions of the vascular basement membrane are multilayered (**B** and **C**, **arrows**). By contrast, the basement membrane on tumor cell clusters is uniformly thin, compact, and closely apposed to tumor cells (**A**, **arrowheads**). RBC, extravasated erythrocytes. Scale bar, 2.5 μm (**A**); 1 μm (**B**, **C**).

the vascular basement membrane were evident, including a loose association with endothelial cells and pericytes, variable thickness, multiple redundant layers, and projections into the perivascular stroma. Basement membrane also covered endothelial sprouts and, in association with pericytes, extended beyond the CD31-positive tip of most sprouts. Basement membrane on clusters of tumor cells did not exhibit these abnormalities.

Distribution of Endothelial Cell and Basement Membrane Markers of Tumor Vessels

CD31, endoglin, VEGFR-2, and integrin alpha5, which are recognized markers of endothelial cells in tumors,[31–33] primarily co-localized on tumor vessels in our studies. Integrin alpha5 was included because it is the receptor for the basement membrane marker fibronectin.[33] None of these markers identified more vessels than CD31. These findings are consistent with published data from the same three tumors showing that all functional blood vessels identified by lectin perfusion had CD31 immunoreactivity.[34] Focal regions—probably individual endothelial cells—of some vessels in LS174T human colon carcinomas implanted in mice lack immunoreactivity for both CD31 and endoglin.[6] Such mosaic vessels may have scattered endothelial cells that do not express these markers or even regions lacking endothelial cells.[6] Blood vessels in uveal melanomas and certain other human and

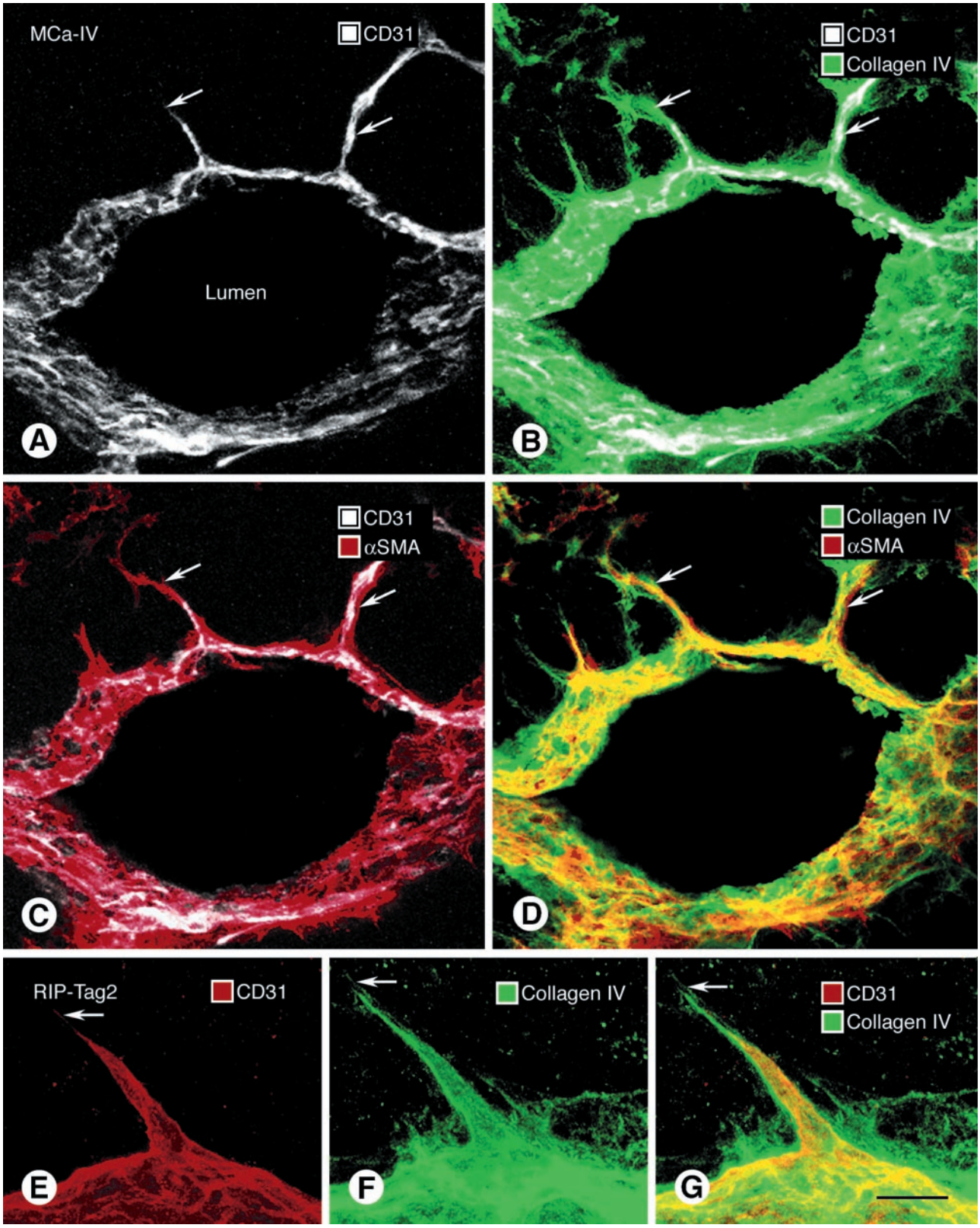

Figure 7. Relationship of basement membrane (type IV collagen immunoreactivity, green), endothelial cells (CD31 immunoreactivity, white), and pericytes (α-SMA immunoreactivity, red) in vascular sprouts (**arrows**) in 80-μm-thick sections of MCa-IV tumor (**A–D**) and RIP-Tag2 tumor (**E–G**). Vessel in **A–D** cut obliquely. The tip of CD31-stained sprouts (**A**, **E**) ends short of the distal-most extension of type IV collagen immunoreactivity (**B**, **F**, **G**) and α-SMA immunoreactivity (**C**). However, type IV collagen staining coincides with the α-SMA immunoreactivity of pericyte processes on the sprouts (**D**). Scale bar, 50 μm (**A–D**); 5 μm (**E–G**).

Table 2. Basement Membrane Coverage of Endothelial Sprouts on Tumor Blood Vessels*

	RIP-Tag2 pancreatic islet tumors	MCa-IV mammary carcinomas	Lewis lung carcinomas
Length of CD31-immunoreactive endothelial sprouts (range)	13 ± 1 μm (5–35 μm)	32 ± 5 μm (11–61 μm)	20 ± 4 μm (5– 49 μm)
Length of type IV collagen-immunoreactive sleeve on endothelial sprouts (range)	23 ± 2 μm (7–41 μm)	54 ± 9 μm (14–90 μm)	30 ± 5 μm (9–75 μm)
Length of portion of type IV collagen-immunoreactive sleeve beyond tip of CD31-staining	10 ± 3 μm	22 ± 3 μm	10 ± 3 μm
Length of type IV collagen-immunoreactive sleeve on endothelial sprouts expressed as % of length of CD31-stained sprout	175 ± 18%	170 ± 7%	153 ± 18%
Length of pericyte processes on sprouts expressed as % of length of CD31-stained sprout†	180%	162%	138%
Percent of sprouts with naked tips (length of naked tips of sprouts)	5% (4.8 μm)	5% (5.5 μm)	5% (4.2 μm)

*Endothelial sprouts, identified as thin, tapered, blind-ended CD31-immunoreactive projections away from the vascular axis, were analyzed in 80-μm sections of tumors double-stained for type IV collagen and CD31 immunoreactivities. Naked tips represent the distal-most region of CD31 staining of sprouts with no detectable type IV collagen immunoreactivity. No sprouts were identified on blood vessels of normal pancreatic islets. Values are expressed as means ± SE (n = 4 mice per group). Ten sprouts were examined in each mouse. Ranges are values for 40 sprouts per group.
†Pericyte data from Morikawa et al. (2002).[10]

experimental tumors have been reported to lack endothelial cells altogether (vasculogenic mimicry) but are lined by periodic acid-Schiff-positive basement membrane.[35] Although these issues were not specifically addressed in the present study, the near perfect correspondence between type IV collagen and CD31 immunoreactivities weighs against vasculogenic mimicry playing a role in the tumor models studied. Blood lakes in RIP-Tag2 tumors contain erythrocytes surrounded by tumor cells but are not surrounded by endothelial cells or basement membrane and are not connected to the bloodstream.[7]

Type IV collagen, laminin, fibronectin, and entactin/nidogen are major protein components of the basement membrane of normal blood vessels.[36] Some studies have examined the distribution of one or more of these markers on tumor vessels.[17,18,28–30] However, the co-localization of multiple basement membrane proteins specifically with endothelial cells of tumor vessels has received less attention.[28] In the three tumor models examined, most of the type IV collagen immunoreactivity was associated with blood vessels, as indicated by its juxtaposition to CD31 and α-SMA immunoreactivities. Entactin/nidogen, laminin, and fibronectin immunoreactivities were also clearly associated with tumor vessels but their presence elsewhere in tumors made them less useful for assessing vascular basement membrane in the tumor models examined.

Our finding that almost the entire surface of tumor blood vessels was covered with type IV collagen immunoreactivity came as a surprise, because of reports that the basement membrane on tumor vessels is incomplete.[24,25,27] Some evidence that tumor vessels have an incomplete or no basement membrane has come from electron microscopic observations.[25,26] Ultrastructural studies typically examine very thin (50 to 100 nm) sections, and visualization of basement membranes is dependent on binding of heavy metals (osmium, lead, uranium) that give electron density to the tissue. Basement membrane on some tumor vessels may not be stained or recognizable by EM.[25,30] Also, the resolution of EM is high, but sampling is limited, and the overall amount of basement membrane coverage of the vessel surface is difficult to estimate. By comparison, the immunoreactivity of specific basement membrane proteins in 1-μm optical slices obtained by confocal microscopy of 80-μm physical sections of tumors provided an opportunity to examine the entire circumference of many tumor vessels. Although tiny defects—perhaps visible by EM—may be missed, the approach did give an overview and made it possible to calculate that on average only 0.03% of the endothelial surface was devoid of type IV collagen immunoreactivity in the tumor models examined. This value was in the same range as found on blood vessels of normal pancreatic islets.

Several additional factors may contribute to the discrepancy between the present results and certain previous findings. Human tumors may be years old and exposed to chemotherapy or radiotherapy before being examined, but little is known of the effects of age or treatment on the vascular basement membrane. Further, the immunohistochemical staining and ultrastructure of human tumors obtained postmortem and processed by standard methods may differ from experimental tumors optimally fixed by vascular perfusion to preserve blood vessels in an open state and to maintain the natural relationship of the basement membrane with endothelial cells and pericytes.

Defects in Endothelial Cells and Basement Membrane of Tumor Blood Vessels

Focal defects in CD31 immunoreactivity, coinciding with defects in type IV collagen immunoreactivity, may represent holes in the endothelium. Intercellular openings observed by scanning EM constitute ~0.1% of the endothelial surface in MCa-IV tumors.[7] This value is in scale with the proportion of vessel surface lacking type IV collagen immunoreactivity in MCa-IV tumors (0.05%, Ta-

ble 1). Thus, some focal sites devoid of CD31 and type IV collagen immunoreactivities are likely to represent endothelial defects that are sites of leakage.[7] However, not all defects in CD31 immunoreactivity were next to corresponding defects in type IV collagen immunoreactivity and vice versa. Whatever the explanation of these defects, their small size indicates pathology at a subcellular scale rather than the presence of mosaic or missing endothelial cells.[6]

Abnormal Morphology of Basement Membrane on Tumor Blood Vessels

Basement membrane on blood vessels in the three tumor models was loosely associated with endothelial cells and pericytes, was irregular in thickness, had multiple layers and other redundancies, and invaded the tumor stroma or parenchyma in some regions. All of these features are consistent with the unstable or dynamic nature of tumor vessels. Some of these abnormalities are not unique to tumors, as they are found in blood vessels in degenerating and regenerating tissues. The tunica vasculosa lentis of the lens is a well-studied site of blood vessel degeneration. Approximately at the time of birth or soon thereafter, the endothelial cells of these vessels regress, leaving empty sleeves of basement membrane, designated intercapillary strands, that persist for several days thereafter.[37,38] Similarly, in the degenerating ovarian corpus luteum, regressing velum of tadpoles during metamorphosis, and tumors treated with angiogenesis inhibitors, endothelial cells detach from their basement membrane, leaving strands of basement membrane devoid of endothelial cell coverage.[39–41]

These situations are reminiscent of the regions of type IV collagen immunoreactivity that are not immediately next to endothelial cells in the tumors we examined. It has been known for many years that basement membrane is ruffled on degenerating capillaries, nerve fibers, and skeletal muscle cells, and can survive long after the underlying cells die.[42,43] Furthermore, the underlying cells can regenerate along the surviving basement membrane that acts as a template or scaffold[42] as for regenerating axons.[43] Regenerating capillaries may have multilayered basement membranes[42] similar to those we and others[44] have observed in tumors. Another example of multilayered vascular basement membrane is found on corneal vessels that survive removal of a growth factor-containing pellet implanted to stimulate angiogenesis.[45] Thus, the basement membrane abnormalities described are not unique to tumor vessels. The notion that some components of the basement membrane of tumor vessels do not have a stable relationship with endothelial cells or pericytes is consistent with the dynamic nature of the tumor vasculature.

Basement Membrane on Endothelial Sprouts

Another surprising finding in our study was the complete coverage of most endothelial sprouts by basement membrane. Angiogenesis may start with the degradation of vascular basement membrane of parent vessels.[20,46,47] On the other hand, there are reports that endothelial sprouts are coated by basement membrane at the outset.[21–23] Our findings are consistent with the latter observations. An alternative interpretation is that pericytes, enveloped by basement membrane, may guide the growth of endothelial sprouts.[48] Indeed, pericytes are located on sprouts,[10,49] contribute to the synthesis of basement membrane on blood vessels,[50] and were associated with most of the sprouts we observed.

A related question is whether the endothelial sprouts observed in tumors actually represent sites of blood vessel growth. The very term sprout implies that endothelial cells are growing, but this assumption is difficult to verify solely on the basis of static images of fixed tissues.[49] Our quantitative data on the cellular composition of sprouts provide some clues. In most sprouts, the basement membrane and pericyte processes were approximately the same length and both were longer than the endothelial cell portion. Furthermore, our earlier study showed that the vascular lumen of sprouts was shorter than the CD31-immunoreactive endothelial cells.[10] These features of endothelial sprouts on tumor vessels could be explained by pericytes forming the basement membrane at the tip of sprouts, ahead of advancing endothelial cell processes. Alternatively, the endothelial cell portion of sprouts may reach the tip but lack CD31 immunoreactivity and a lumen. Some sprouts may instead be retracting, with the endothelial cell portion moving faster than the pericytes or basement membrane. Realistically, multiple processes are likely to occur concurrently, as blood vessels in tumors are in a constant state of flux, sometimes growing and sometimes regressing.[51] Studies of the effects of angiogenesis inhibitors should help to elucidate the relative contributions of the various mechanisms involved.

One motivation for studying the basement membrane of tumor vessels stems from its use as a target for diagnostic or therapeutic agents.[12] Disruption of their contact with basement membrane can lead to endothelial cells' apoptosis and tumor regression.[52–54] Evidence that basement membrane can store growth factors[55,56] and is a source of angiogenic[14,57] and anti-angiogenic factors[13,15] adds to the importance of understanding the peculiar features of the basement membrane of tumor vessels.

Conclusions

Blood vessels in the three mouse tumor models we studied are almost completely covered by basement membrane, as detected by type IV collagen, entactin/nidogen, laminin, and fibronectin immunoreactivities. Basement membrane defects are at most a few micrometers in diameter and expose less than 0.1% of the vessel surface, which is similar to normal vessels. However, the vascular basement membrane in tumors has conspicuous abnormalities, including irregular thickness, multiple layers, and loose association with endothelial cells and pericytes, reminiscent of degenerating or regenerating blood vessels. Basement membrane also covers most

endothelial sprouts. These features of the vascular basement membrane are consistent with the dynamic nature of endothelial cells and pericytes in tumors.

Acknowledgments

We thank Tetsuichiro Inai for helpful discussions; Douglas Hanahan for providing breeding pairs for our colony of RIP-Tag2 mice; Carolyn Woo and Erin Ator for animal care; Gyulnar Baimukanova for genotyping the mice; Rakesh Jain and Sylvie Roberge of the Massachusetts General Hospital, Boston, MA, for supplying the MCa-IV tumors; and Rolf Brekken of the Hope Heart Institute, Seattle, WA, for the kind gift of antibody to VEGFR-2.

References

1. Pasqualini R, Arap W, McDonald DM: Probing the structural and molecular diversity of tumor vasculature. Trends Mol Med 2002, 8:563–571
2. St. Croix B, Rago C, Velculescu V, Traverso G, Romans KE, Montgomery E, Lal A, Riggins GJ, Lengauer C, Vogelstein B, Kinzler KW: Genes expressed in human tumor endothelium. Science 2000, 289: 1197–1202
3. Folkman J: Angiogenesis-dependent diseases. Semin Oncol 2001, 28:536–542
4. Jain RK: Normalizing tumor vasculature with anti-angiogenic therapy: a new paradigm for combination therapy. Nat Med 2001, 7:987–989
5. Warren BA: The vascular morphology of tumors. Tumor Blood Circulation. Edited by HE Peterson. Boca Raton, CRC Press Inc., 1979, pp 1–48
6. Chang YS, di Tomaso E, McDonald DM, Jones R, Jain RK, Munn LL: Mosaic blood vessels in tumors: frequency of cancer cells in contact with flowing blood. Proc Natl Acad Sci USA 2000, 97:14608–14613
7. Hashizume H, Baluk P, Morikawa S, McLean JW, Thurston G, Roberge S, Jain RK, McDonald DM: Openings between defective endothelial cells explain tumor vessel leakiness. Am J Pathol 2000, 156: 1363–1380
8. Eberhard A, Kahlert S, Goede V, Hemmerlein B, Plate KH, Augustin HG: Heterogeneity of angiogenesis and blood vessel maturation in human tumors: implications for antiangiogenic tumor therapies. Cancer Res 2000, 60:1388–1393
9. Abramsson A, Berlin O, Papayan H, Paulin D, Shani M, Betsholtz C: Analysis of mural cell recruitment to tumor vessels. Circulation 2002, 105:112–117
10. Morikawa S, Baluk P, Kaidoh T, Haskell A, Jain RK, McDonald DM: Abnormalities in pericytes on blood vessels and endothelial sprouts in tumors. Am J Pathol 2002, 160:985–1000
11. Gee MS, Procopio WN, Makonnen S, Feldman MD, Yeilding NM, Lee WM: Tumor vessel development and maturation impose limits on the effectiveness of anti-vascular therapy. Am J Pathol 2003, 162:183–193
12. Neri D, Carnemolla B, Nissim A, Leprini A, Querze G, Balza E, Pini A, Tarli L, Halin C, Neri P, Zardi L, Winter G: Targeting by affinity-matured recombinant antibody fragments of an angiogenesis associated fibronectin isoform. Nature Biotechnol 1997, 15:1271–1275
13. Marneros AG, Olsen BR: The role of collagen-derived proteolytic fragments in angiogenesis. Matrix Biol 2001, 20:337–345
14. Xu J, Rodriguez D, Petitclerc E, Kim JJ, Hangai M, Moon YS, Davis GE, Brooks PC, Yuen SM: Proteolytic exposure of a cryptic site within collagen type IV is required for angiogenesis and tumor growth in vivo. J Cell Biol 2001, 154:1069–1079
15. Kalluri R: Basement membranes: structure, assembly and role in tumor angiogenesis. Nat Rev Cancer 2003, 3:422–433
16. Yurchenco PD, O'Rear J: Supramolecular organization of basement membranes. Molecular and Cellular Aspects of Basement Membranes. Edited by DH Rohrbach, R Timpl. San Diego, Academic Press, 1993, pp 19–47
17. Paulus W, Roggendorf W, Schuppan D: Immunohistochemical investigation of collagen subtypes in human glioblastomas. Virchows Arch A Pathol Anat Histopathol 1988, 413:325–332
18. Hewitt RE, Powe DG, Morrell K, Balley E, Leach IH, Ellis IO, Turner DR: Laminin and collagen IV subunit distribution in normal and neoplastic tissues of colorectum and breast. Br J Cancer 1997, 75:221–229
19. Inoue S: Ultrastructure of basement membranes. Int Rev Cytol 1989, 117:57–98
20. Kalebic T, Garbisa S, Glaser B, Liotta LA: Basement membrane collagen: degradation by migrating endothelial cells. Science 1983, 221:281–283
21. Jerdan JA, Michels RG, Glaser BM: Extracellular matrix of newly forming vessels—an immunohistochemical study. Microvasc Res 1991, 42:255–265
22. Gusterson BA, Warburton MJ, Mitchell D, Kraft N, Hancock WW: Invading squamous cell carcinoma can retain a basal lamina. An immunohistochemical study using a monoclonal antibody to type IV collagen. Lab Invest 1984, 51:82–87
23. Egginton S, Zhou AL, Brown MD, Hudlicka O: Unorthodox angiogenesis in skeletal muscle. Cardiovasc Res 2001, 49:634–646
24. Steinberg F, Konerding MA, Streffer C: The vascular architecture of human xenotransplanted tumors: histological, morphometrical, and ultrastructural studies. J Cancer Res Clin Oncol 1990, 116:517–524
25. Paku S, Paweletz N: First steps of tumor-related angiogenesis. Lab Invest 1991, 65:334–346
26. Nakanishi H, Okayama M, Oguri K, Hayashi K, Tateno H, Hosoda S: Close association between tumour cells and vascular basement membrane in gastric cancers with liver metastasis. An immunohistochemical and electron microscopic study with special attention to extracellular matrices. Virchows Arch A Pathol Anat Histopathol 1991, 418:531–538
27. Paku S: Current concepts of tumor-induced angiogenesis. Pathol Oncol Res 1998, 4:62–75
28. Farnoud MR, Lissak B, Kujas M, Peillon F, Racadot J, Li JY: Specific alterations of the basement membrane and stroma antigens in human pituitary tumours in comparison with the normal anterior pituitary. An immunocytochemical study. Virchows Arch A Pathol Anat Histopathol 1992, 421:449–455
29. Murray JC, Smith KA, Lauk S: Vascular markers for murine tumours. Radiother Oncol 1989, 16:221–234
30. Eyden B, Yamazaki K, Menasce LP, Charchanti A, Agnantis NJ: Basement-membrane-related peri-vascular matrices not organised as a basal lamina: distribution in malignant tumours and benign lesions. J Submicrosc Cytol Pathol 2000, 32:515–523
31. Fonsatti E, Altomonte M, Arslan P, Maio M: Endoglin (CD105): a target for anti-angiogenetic cancer therapy. Curr Drug Targets 2003, 4:291–296
32. Brekken RA, Thorpe PE: Vascular endothelial growth factor and vascular targeting of solid tumors. Anticancer Res 2001, 21:4221–4229
33. Kim S, Bell K, Mousa SA, Varner JA: Regulation of angiogenesis in vivo by ligation of integrin alpha5beta1 with the central cell-binding domain of fibronectin. Am J Pathol 2000, 156:1345–1362
34. Morikawa S, Baluk P, Jain RK, McDonald DM: Abnormal basal lamina and abundant pericytes on tumor vessels. Proc Am Assoc Cancer Res 2001, 42:565
35. Maniotis AJ, Folberg R, Hess A, Seftor EA, Gardner LM, Pe'er J, Trent JM, Meltzer PS, Hendrix MJ: Vascular channel formation by human melanoma cells in vivo and in vitro: vasculogenic mimicry. Am J Pathol 1999, 155:739–752
36. Paulsson M: Basement membrane proteins: structure, assembly, and cellular interactions. Crit Rev Biochem Mol Biol 1992, 27:93–127
37. Latker CH, Kuwabara T: Regression of the tunica vasculosa lentis in the postnatal rat. Invest Ophthalmol Vis Sci 1981, 21:689–699
38. el-Hifnawi E, el-Hifnawi A, Frankenberg C, Keeler C: Ultrastructure and regression of the tunica vasculosa lentis in newborn Wistar rats. Anat Anz 1994, 176:143–149
39. Modlich U, Kaup FJ, Augustin HG: Cyclic angiogenesis and blood vessel regression in the ovary: blood vessel regression during luteolysis involves endothelial cell detachment and vessel occlusion. Lab Invest 1996, 74:771–780
40. Bartel H, Lametschwandtner A: Regression of blood vessels in the ventral velum of Xenopus laevis Daudin during metamorphosis: light

microscopic and transmission electron microscopic study. J Anat 2000, 197:157–166
41. McDonald DM, Choyke PL: Imaging of angiogenesis: from microscope to clinic. Nat Med 2003, 9:713–725
42. Vracko R: Basal lamina scaffold-anatomy and significance for maintenance of orderly tissue structure. Am J Pathol 1974, 77:314–346
43. Ide C: Nerve regeneration and Schwann cell basal lamina: observations of the long-term regeneration. Arch Histol Jpn 1983, 46:243–257
44. Giordana MT, Germano I, Giaccone G, Mauro A, Migheli A, Schiffer D: The distribution of laminin in human brain tumors: an immunohistochemical study. Acta Neuropathol (Berl) 1985, 67:51–57
45. Ausprunk DH, Falterman K, Folkman J: The sequence of events in the regression of corneal capillaries. Lab Invest 1978, 38:284–294
46. Vlodavsky I, Ariav Y, Atzmon R, Fuks Z: Tumor cell attachment to the vascular endothelium and subsequent degradation of the subendothelial extracellular matrix. Exp Cell Res 1982, 140:149–159
47. Glaser BM, Kalebic T, Garbisa S, Connor TB, Liotta LA: Degradation of basement membrane components by vascular endothelial cells: role in neovascularization. Ciba Found Symp 1983, 100:150–162
48. Nehls V, Denzer K, Drenckhahn D: Pericyte involvement in capillary sprouting during angiogenesis in situ. Cell Tissue Res 1992, 270: 469–474
49. Hashizume H, Ushiki T: Three-dimensional cytoarchitecture of angiogenic blood vessels in a gelatin sheet implanted in the rat skeletal muscular layers. Arch Histol Cytol 2002, 65:347–357
50. Jeon H, Ono M, Kumagai C, Miki K, Morita A, Kitagawa Y: Pericytes from microvessel fragment produce type IV collagen and multiple laminin isoforms. Biosci Biotechnol Biochem 1996, 60:856–861
51. Brown EB, Campbell RB, Tsuzuki Y, Xu L, Carmeliet P, Fukumura D, Jain RK: In vivo measurement of gene expression, angiogenesis and physiological function in tumors using multiphoton laser scanning microscopy. Nat Med 2001, 7:864–868
52. Ingber DE, Madri JA, Folkman J: A possible mechanism for inhibition of angiogenesis by angiostatic steroids: induction of capillary basement membrane dissolution. Endocrinology 1986, 119:1768–1775
53. Brooks PC, Montgomery AM, Rosenfeld M, Reisfeld RA, Hu T, Klier G, Cheresh DA: Integrin alpha v beta 3 antagonists promote tumor regression by inducing apoptosis of angiogenic blood vessels. Cell 1994, 79:1157–1164
54. Liu W, Ahmad SA, Reinmuth N, Shaheen RM, Jung YD, Fan F, Ellis LM: Endothelial cell survival and apoptosis in the tumor vasculature. Apoptosis 2000, 5:323–328
55. Folkman J, Klagsbrun M, Sasse J, Wadzinski M, Ingber D, Vlodavsky I: A heparin-binding angiogenic protein—basic fibroblast growth factor—is stored within basement membrane. Am J Pathol 1988, 130: 393–400
56. Bergers G, Brekken R, McMahon G, Vu TH, Itoh T, Tamaki K, Tanzawa K, Thorpe P, Itohara S, Werb Z, Hanahan D: Matrix metalloproteinase-9 triggers the angiogenic switch during carcinogenesis. Nat Cell Biol 2000, 2:737–744
57. Brooks PC: Cell adhesion molecules in angiogenesis. Cancer Metastasis Rev 1996, 15:187–194